Bioprocess and Biosystems Engineering (2024) 47:737–751
https://doi.org/10.1007/s00449-024-03010-7

RESEARCH PAPER

Evaluation of free and immobilized cellulase on chitosan-modified magnetic nanoparticles for saccharification of sorghum residue

Pallavi Punia[1] · **Lakhvinder Singh**[1]

Received: 5 January 2024 / Accepted: 27 March 2024 / Published online: 12 April 2024

Abstract

Enzymatic hydrolysis plays a pivotal role in transforming lignocellulosic biomass. Addressing alternate techniques to optimize the utilization of cellulolytic enzymes is one strategy to improve its efficiency and lower process costs. Cellulases are highly specific and environmentally benign biocatalysts that break down intricate polysaccharides into simple forms of sugars. In contrast to the most difficult and time-consuming enzyme immobilization processes, in this research, we studied simple, mild, and successful techniques for immobilization of pure cellulase on magnetic nanocomposites using glutaraldehyde as a linker and used in the application of sorghum residue biomass. Fe_3O_4 nanoparticles were coated with chitosan from the co-precipitation method, which served as an enzyme carrier. The nanoparticles were observed under XRD, Zeta Potential, FESEM, VSM, and FTIR. The size morphology results presented that the Cs@Fe_3O_4 have 42.2 nm, while bare nanoparticles (Fe_3O_4) have 31.2 nm in size. The pure cellulase reaches to 98.07% of loading efficiency and 71.67% of recovery activity at optimal conditions. Moreover, immobilized enzyme's pH stability, thermostability, and temperature tolerance were investigated at suitable conditions. The kinetic parameters of free and immobilized enzyme were estimated as V_{max}; 29 ± 1.51 and 27.03 ± 2.02 µmol min^{-1} mg^{-1}, K_m; 4.7 ± 0.49 mM and 2.569 ± 0.522 mM and K_{cat}; 0.13 s^{-1}, and 0.89 s^{-1}. Sorghum residue was subjected to 2% NaOH pre-treatment at 50 ℃. Pre-treated biomass contains cellulose of 64.8%, used as a raw material to evaluate the efficiency of reducing sugar during hydrolysis and saccharification of free and immobilized cellulase, which found maximum concentration of glucose 5.42 g/L and 5.12 g/L on 72 h. Thus, our study verifies the use of immobilized pure cellulase to successfully hydrolyze raw material, which is a significant advancement in lignocellulosic biorefineries and the reusability of enzymes.

Keywords Sweet sorghum residue · Nanoparticles · Immobilization · Enzymatic hydrolysis · Enzyme kinetics

Introduction

To address fossil fuel depletion and mitigate its associated drawbacks, it is imperative to provide a dependable and environmentally friendly alternative energy source. Among the aforementioned alternate sources, biofuels emerge as the most viable kind. Biomass composed of lignocellulose is being considered as a potential renewable asset for biofuel production. It can potentially improve the food-to-fuel ratio and provide sufficient feedstock for biofuel generation [1]. In the series of production of bioethanol, lignocellulosic biomass comprises carbohydrates consisting of hetero-polymeric molecules such as cellulose or hemicellulose, which are further hydrolyzed to produce fermentable sugars and then reduced sugars fermented to alcohol. Production of biofuel from suitable feedstocks is a challenging task. Selection of appropriate feedstocks and efficient microorganisms which help in fermentation is continuous topic of research. The sweet sorghum plant, also known as *Sorghum bicolor* (L.) *Moench*, is one of the noteworthy feedstocks utilized in the manufacturing of bioethanol [2, 3]. An essential herbaceous crop growing in tropical and equatorial climates, sweet sorghum is a C4 plant. Just over a quarter of the water needed to cultivate sugarcane was used by sweet sorghum residue plantations. This crop can boost bioethanol production in regions where sugarcane or crop varieties

✉ Lakhvinder Singh
lakhvinder16@gmail.com

Pallavi Punia
pallavipunia28@gmail.com

[1] Department of Environmental Science and Engineering, Guru Jambheshwar University of Science and Technology, Hisar 125001, Haryana, India

are not doing well since it can be grown in drier conditions [4, 5]. If the collaborative approach is economically viable, the biomass from sweet sorghum production must be acceptable for use as a raw material in value-added goods; otherwise, it will result in a new sorghum bagasse residue. Research suggests utilizing the sweet sorghum's biomass to enhance land-based crop use [6]. This sorghum variety has been significantly studied for its ability to thrive in various climates and its resilience to drought. A significant quantity of lignocellulosic residue remains as a waste product of sweet sorghum, referred to as residue. This residue is the sole non-food application component of the crop that may be utilized as a potential solution for addressing the issue of food-versus-fuel ratio [7, 8]. Literature study by Verma et al. [9] illustrates that one of the most prominent foundations for feasible energy sources is the biomass composed of lignocellulose. The breakdown of lignocellulosic biomass that was in use for the manufacture of biofuel was typically accomplished through the utilization of a variety of standard pre-treatment techniques. A straightforward and effective method for improving biomass's ability to be absorbed was to subject it to chemical pre-treatment using acid, alkali, or oxidative chemicals. The biomass structure was subjected to pre-treatments to facilitate the eradication of lignin from the substrate. This process enables the efficient conversion of cellulose into fermentable sugars by enzymatic hydrolysis [10]. Alkali pre-treatment has gained substantial prominence in recent years due to its favorable characteristics, including mild conditions, little constraints for subsequent treatment, low energy consumption, and cost-effectiveness. These attributes make it a very impacting technology for many agricultural feedstocks. Concurrently, a significant mechanism of alkali pre-treatment involves the degradation of ester bonds within the lignocellulosic cell wall, leading to the cleavage of glycosidic chains. This process has an impact on the lignin cord, resulting in arise in cellulose crystallinity. Consequently, the viability of cellulose is enhanced, and the structural linkages are agitated, ultimately resulting in an increased yield of saccharification [11]. In the alkali pre-treatment for biofuel production, sodium hydroxide (NaOH) has potential approach. The main reason behind this approach is that NaOH can break the ester bond between hemicellulose and lignin and increase cellulose concentration in the liquid phase [12, 13]. The degradation of compounds during alkali pre-treatment can enhance ethanol's enzymatic saccharification and fermentation [14].

Conversely, enzymatic hydrolysis is typically performed in mild circumstances (pH 4.5–5, temperature 45–50 ℃) and does not pose any issue with material corrosion [15]. For many biological and chemical processes, enzymes are the most effective catalysts. A higher cellulose concentration remains after pre-treatment, making hydrolysis into the oligosaccharide glucose amenable. After pre-treating biomass for simple hydrolysis, these enzymes can be utilized efficiently to make a biofuel of preference [16]. Enzyme immobilization strategies are used to overcome the problem that would arise in the context of the long-term stability of enzymes, their reusability and recovery. When enzymes are immobilized on solid supports, the catalytic properties of enzymes are altered, modifying their reusability, chances of proper selectivity, and shell life [17, 18].

The use of nanotechnology has transformed enzyme immobilization techniques by offering diverse nanomaterials. Biodegradable nanomaterial is a new type of support for immobilizing lipase enzyme to improve biodiesel synthesis. When it came to biodiesel manufacturing, the immobilized enzyme had a far higher transesterification yield (90%) than the free lipase (74%) stated by Verma and Borrow [19]. Similar findings by Verma et al. [20] demonstrated the effective and sustainable generation of biodiesel from algal-based nanoparticles by immobilized the lipase enzyme. The immobilization of enzymes on various nanomaterials, including nanofibers and nano-polymers, increases research interest in this field [21, 22]. Among these nanomaterials, metal oxide nanoparticles, such as Fe_3O_4, NiO_2, titanium oxide, etc. support immobilization. Magnetic nanoparticles have great advancements for immobilizing enzymes because they provide a greater surface area for enzymatic reactions and magnetic properties, so the recovery of enzymes would be easy by applying a magnetic field [23, 24]. Various techniques can be used for immobilization, among which physical adsorption and covalent bonding are widely used. Physical adsorption framed the interactions between Van der Waals force and hydrogen bonding between enzymes and solid support. Covalent bonding, where covalent bonds can combine bioactive material with solid support [25–28]. Surface modification on nanoparticles enhances their efficiency and increases the ratio of surface to volume for further evaluation. Chitosan is a biopolymer comprising poly (1–4)-2-amino-2-deoxy-D-glucose, which is environment-safe. Modification of chitosan on magnetic nanoparticle support will lay out biocompatibility for the system [29, 30]. Various studies also reveal that many carbohydrate nanomaterials acquired from biopolymers like chitosan and alginate are stepped out the current trends in patents awarded for biotechnological applications are analyzed, coupled with a discussion on their attractive prospects stated by Verma et al. [31]. Iron-magnetic nanoparticles are modified by immobilizing the cellulase enzyme on chitosan scaffolding. Enzymes may be readily obtained due to the presence of many functional structures, involving as hydroxymethyl, amino, and hydroxyl groups, in $Cs@Fe_3O_4$ [32, 33]. Verma et al. [34] suggested the applications of graphene-based biosensors in various biotechnology fields. Also, they stated that the enzymatic sensors were used to detect glucose, phenols, hydrogen peroxide etc.

Glutaraldehyde was used as the cross-linking agent to connect the enzyme to the firm base. We can preserve the enzyme's functional and structural properties using GA as an adhesive agent. Enzymes attached to magnetic nanoparticles are covalently cross-linked by glutaraldehyde [35]. To determine if the modified magnetic nanoparticle support can load enzymes, ideal circumstances must be met, including temperature, pH, thermal stability, and reusability. Literature studies by Verma et al. [36] proposed the various enzymes immobilized on chitosan bi-polymer with the support of glutaraldehyde carrier for several biotechnological applications like sustainable agricultural uses, biofuel production, etc.

Saccharomyces cerevisiae is commonly utilized in fermentation due to its inherent capacity to generate high ethanol production and output. Additionally, it is a thermotolerant yeast capable of surviving in harsh environments. But the major drawback of *S. cerevisiae* yeast is that it can only convert simple sugars like glucose and sucrose to biofuel [37]. For hexose and pentose sugars, yeast can be used, i.e., *Pichia stipitis.* Simultaneously cultivating both types of yeast throughout the fermentation process improved biofuel output and yield percentage [38].

This research aimed to immobilize the cellulase enzyme complex on chitosan-coated Fe_3O_4 nano-support by co-precipitation. It obtained nanoparticles characterized by FTIR (Fourier transforms infrared spectroscopy), XRD, FESEM (scanning electron microscopy), Zeta potential, and VSM (vibrating sampler magnetometer). This study also investigated the glucose yield obtained during hydrolysis of sweet sorghum residue from immobilized enzyme and free enzyme and also used starting material for saccharification for obtaining by-product. The hydrolyzing capacity of immobilized cellulase on sweet sorghum bagasse was investigated to produce reducing sugar by saccharification. Because the highly effective magnetic nanocomposite is readily separated, it facilitates the reutilization of cellulase over numerous hydrolytic cycles, which can directly impact the cost of biofuel production.

Materials and methodology

Materials and chemicals

Ferric chloride hexahydrate ($FeCl_3.6H_2O$) and ferric chloride tetrahydrate ($FeCl_2.4H_2O$) salts, chitosan, glutaraldehyde (GA), and acetic acid solution were acquired from Sigma-Aldrich. Sweet sorghum residue was procured from the local field at Sirsa, Haryana, India. The chemicals used to estimate cellulose and lignin were purchased from Himedia Pvt Ltd, India. Pure Cellulase enzyme was purchased from CDH (Central drug house Pvt Ltd.).

Fe_3O_4 and Cs@Fe_3O_4 nanomaterial synthesis

Nanomaterials with magnetic properties were created by the co-precipitation method using 1:2 ratio of ($FeCl_3.6H_2O$) and ($FeCl_2.4H_2O$) with 100 mL of a 1 M molar (HCl) solution (Fig. 1). Subsequently, 500 mL of ammonium hydroxide (NH_4OH) was added to the combination above in a steady stream while the mixture was vigorously blended at 400 rpm and heated to 70 ℃ until the pH reached 10. After stirring, an instant black precipitate of Fe_3O_4 was obtained. After a 4 h oven drying period at 60 ℃, the iron oxide nanomaterials were allowed to frigid to room temperature for the night. 3.0 g of synthesized Fe_3O_4 nanoparticles dissolved in 50 mL of acetic acid solution containing 2.25 g of chitosan. After adding the chitosan and magnetic nanoparticles, the mixture is rapidly agitated for 20 min to dissolve everything evenly. Subsequently, the combination is subjected to a 1 M NaOH solution, creating Fe_3O_4 nanomaterial covered with chitosan. The functionalized iron nanoparticles underwent many rinses with deionized water until achieving a neutral pH. Subsequently, the nanoparticles were kept at a temperature of 6 ℃ for immobilization.

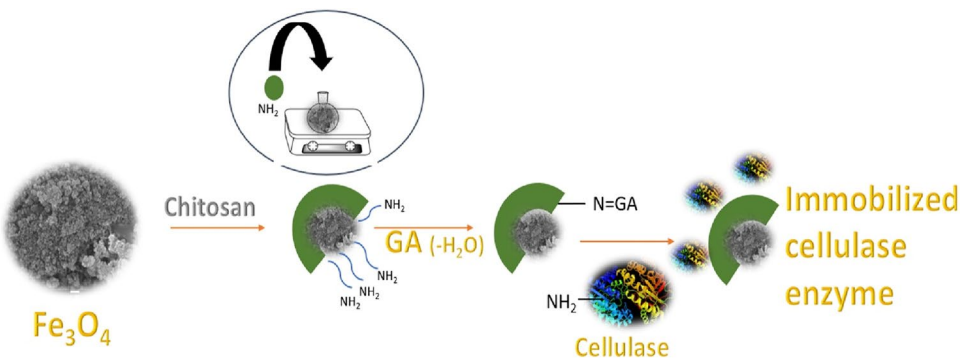

Fig. 1 Fe_3O_4 nanoparticles coated with chitosan and immobilized by enzymes

Chemical and structural characterization of nanoparticles

FTIR characterized the synthesized nanoparticles to govern the changes in functional groups. FTIR spectra were learnt in transmission mode using the KBr background disk method using Perkin Elmer FTIR equipment (Spectrum BX). The surface morphology of iron oxide nanocomposite and functionalized chitosan on nanocomposite adsorbent was studied using a scanning electron microscope (JEOL/7610F plus). Rigaku Miniflex-11 XRD diffractometer scanning in 20–70θ was used to compute crystallinity. At room temperature and with a magnetic field of − 20 to + 20 k O/e, the ferromagnetic properties of the produced nanocomposites of Fe_3O_4/Cs@ Fe_3O_4 were examined using a vibrating sampler magnetometer. Zeta Potential determines the stability of nanomaterials and charges on particular nanomaterial (Fe_3O_4/Ch-MNPs).

Enzymes immobilization

The cellulase enzyme was immobilized using a covalent approach. One-way enzymes were activated was using glutaraldehyde (GA) [39] (Fig. 1). 500 mg of nano-support was dissolved in 50 mL of a 2.0% v/v GA solution to activate aldehyde chains on the scaffold mixture. The combination was then agitated for 3 h at a temperature of 27 °C. Next, this was followed by combining the aforementioned solution with a 100 mg/mL enzyme suspension containing cellulase enzyme and a 0.1 M buffering agent solution. Subsequently, the mixture was subjected to incubation at various temperatures for 2 h. Following removing the supernatant, the immobilized nanoparticles were retrieved by a series of 3–4 washes using deionized water. Protein assay method of Bradford can be used to determine cellulase enzyme's loading efficiency, calculated using the following equation [40].

$$\frac{C_0V_0 - C_1V_1}{C_0V_0} \times 100\% \quad (1)$$

where C_0: protein concentration, V_0: volume of enzyme solution before immobilization.

C_1: protein concentration after immobilization, V_1: after immobilization filtrate volume.

Cellulase enzymatic activity was determined by filter paper activity procedure. Cellulase activity was estimated by Ghose method [41].

Effect of pH and temperature on immobilized and free cellulase

CMC hydrolysis was accomplished at various pH levels (4–8). Several buffers were used in the reactions, such as citrate, phosphate, and acetate buffers, to create substrate and enzymatic solutions, at 50 mM.

The free and immobilized enzyme activity was evaluated throughout a range of temperatures (50–90 °C). Before starting the enzymatic process, enzymes were suspended in acetate buffer 50 mM, pH 4.8 for 10 min at the corresponding temperature. Following each run of the process of hydrolysis, the reactivity of immobilized cellulase was assessed based on its residual CMCase activity, which was reported as relative activity.

Estimation of kinetics parameters of free and immobilized enzyme

Maximal velocity (V_{max}), Michaelis constant (K_m), and catalytic constant (K_{cat}) for both immobilized and free cellulase enzyme samples were calculated at 37 ℃ at pH 8, using CMC as substrate in the range from 0.5 to 2.5 mg/mL. To ascertain the kinetic parameters using given equation, a Lineweaver–Burk plot was generated [42].

$$\frac{1}{V_0} = \frac{K_m}{V_{max}}\left(\frac{1}{[S]}\right) + \frac{1}{V_{max}}$$

Application of immobilized and free cellulase for saccharification and hydrolysis of sweet sorghum residue biomass

A quantity of 1 mm-sized dry sorghum residue was placed in a flask, with a solid waste loading of 10% (w/v). The residue was pre-treated in an autoclave using NaOH at a certain concentration described by Pallavi and Lakhvinder [43]. The composition analysis of pre-treated and un-treated biomass was determined using the method described by the National Renewable Energy Laboratory [44]. Then, the substrate is applied for immobilized enzymatic preparations. The saccharification process with enzymes involved dissolving 1 L of citrate buffer with a pH of 5.0 ± 0.2 in a 200 mL flask containing both free and immobilized cellulase, and in order to suppress the growth of microorganisms in the solution, a concentration of 1.0 mg/mL of sodium azide was added to all experimental flasks at a rotational speed of 180 rpm. Following agitation in the incubator, the mixture was subjected to centrifugation, and the resulting supernatant was collected at various time intervals (24–72 h). The collected supernatant was stored at a temperature of 4 ℃ for the purpose of analyzing reducing sugars [43].

Analysis of reducing sugar

Reducing sugar was estimated using HPLC with a refractive index detector, and Aminex HPX chromatography column

was used for sugar analysis with a flow rate of 1.0 mL/min, injection volume of 10 µL, and a running time of 18 min. Water solution was used for mobile phase. HPLC was calibrated with a standard sugar solution to quantify sugar concentration measurements.

Results and discussion

This study emphasizes on the production and the characterization of magnetite nanoparticles modified with chitosan, along with the immobilization of cellulase enzyme using GA shown in Fig. 1. The term "protonated chitosan" pertains to the introduction of hydrogen cation. Initially dissolved in an acidic solution, Protons are classified as polycations, whereas Fe_3O_4 nanoparticles are regarded as negatively charged. The electrostatic interaction between chitosan and iron oxide nanoparticles is quite strong [45]. The production of Ch-Fe_3O_4 nanoparticles occurred due to the precipitation of chitosan on its surface, which occurred when the pH of the solution was altered to an alkaline state [46]. The covalent linkage of cellulase to the support occurred after the modification of the amino group on the Fe_3O_4–chitosan to an aldehyde cluster by GA, resulting in the immobilization of the enzymes.

Characterization of nanoparticles

The FTIR properties of Fe_3O_4, Cs@Fe_3O_4 and immobilized enzyme on Ch-MNPs are displayed in Fig. 2. The OH group of water is represented by the peaks observed at approximately 3442 cm^{-1} for Fe_3O_4, which shifted to 3455 cm^{-1} in chitosan and 3460 cm^{-1} in immobilized enzyme. The band at 1631 cm^{-1} shows the N–H bending vibration, which shows the chitosan polymer covering on top of Fe_3O_4 nanoparticles. FTIR spectra for immobilized cellulase on Ch-MNPs, in which peaks observed near 1625 cm^{-1} (carbon–oxygen stretching) can be ascribed liaison between carbonyl ester bond of cellulase protein rings and O–H vibration of chitosan-modified iron oxide nanomaterials. Similar results by Jaquelina Sanchez-Ramirez et al. [47] observed the same peaks of CO binding at nearby 1621 cm^{-1} for configuration of immobilization of cellulase on modified chitosan on magnetic nanoparticles. The Fe–O bond in Fe_3O_4 and Cs@Fe_3O_4 displays characteristic bands ranging from 420 cm^{-1} to 630 cm^{-1}. Moreover, a prominent peak at around 556 cm^{-1} in the spectra of enzymes attached to nanoparticles via the Fe–O link signifies the existence of magnetic characteristics.

The XRD patterns of Fe_3O_4 and Cs@Fe_3O_4 are shown in Fig. 3. The XRD spectra of the composites exhibit five distinct peaks corresponding to the planes (220), (311), (400), (422), and (440), respectively, which are characteristic of Fe_3O_4. These peaks demonstrated the spinel structure of produced nanocomposites. The nanoparticles maintained their Fe_3O_4 crystalline structure, as evidenced by identical distinct peaks following chitosan coating. The Fe_3O_4 NPs were auspiciously coated by chitosan, as evidenced by the disappearance of diffraction peaks at $2\theta = 54°$, 71°, and 74°, and a decrease in strength of other diffraction lines [48, 49]. Fe_3O_4 nanoparticles synthesized in this work by the co-precipitation approach exhibited a high level of purity and excellent crystallinity, indicated by an indistinct reflection peak at 18°, indicating the presence of maghemite.

Figure 4 shows the M–H curves of Fe_3O_4 NPs, Cs@Fe_3O_4 NPs and immobilized cellulase at room temperature. The saturation magnetizations (Ms) of Fe_3O_4 nanoparticles, Cs@Fe_3O_4 NPs and Cs@Fe_3O_4@cellulase were measured to be 53.2 emu/g, 47.5 emu/g and 45.2 emu/g, respectively. The integration of chitosan polymer onto Fe_3O_4 NPs resulted in a reduction for the observed saturated magnetization (Ms). This indicates that the magnetite in Cs@Fe_3O_4 NPs has little

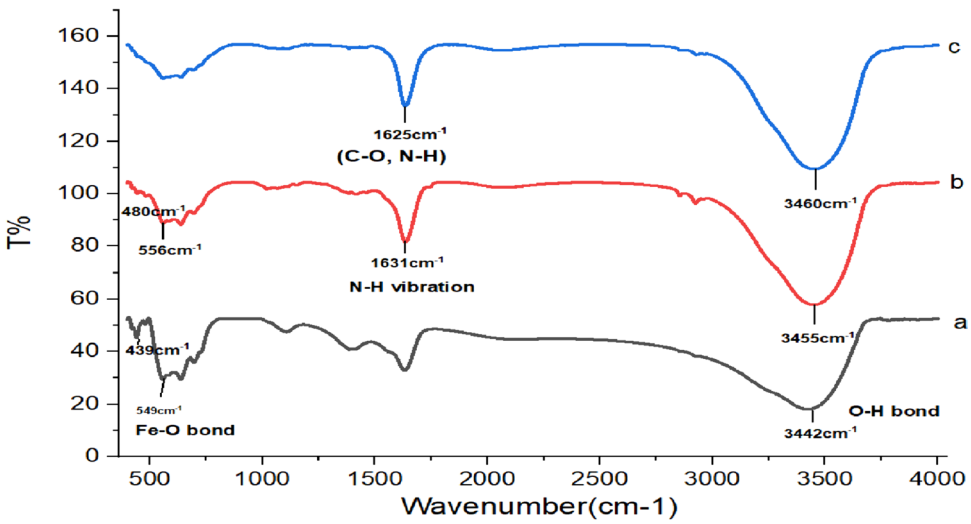

Fig. 2 FTIR spectra of (**a**) Fe_3O_4, (**b**) Cs@Fe_3O_4 and (**c**) immobilized enzyme on Ch-MNPs

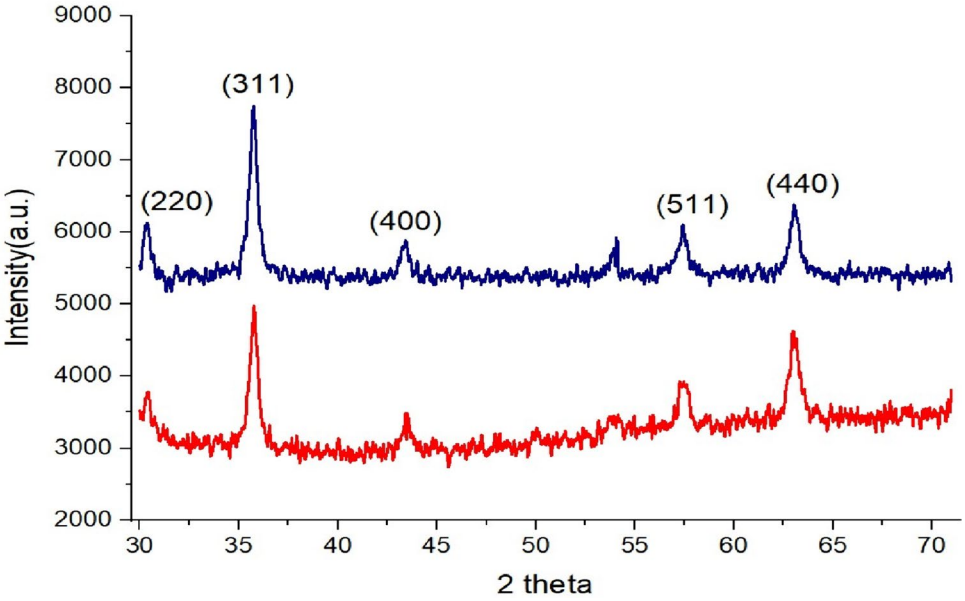

Fig. 3 XRD analysis of Fe_3O_4 (Top line) and $Cs@Fe_3O_4$ (Lower line)

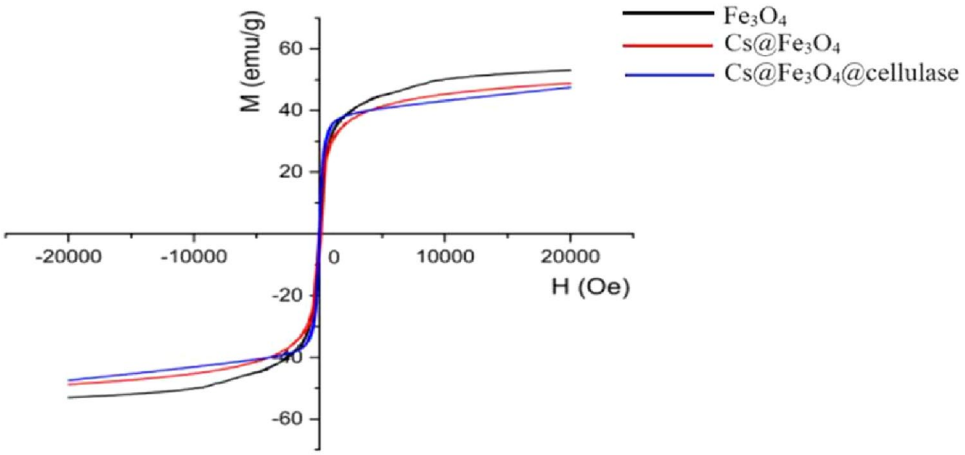

Fig. 4 Magnetization curves for Fe_3O_4 (top line), $Cs@Fe_3O_4$ (middle line) and lower line for $Cs@Fe_3O_4$@cellulase

and an inferior saturation magnetization value. This incident illustrated the ferromagnetic behavior of synthesized magnetic nanoparticles. There is a possibility that the presence of chitosan and laccase adhering to Fe_3O_4 nanoparticles is responsible for the lower magnetization of Fe_3O_4@Cs and $Cs@Fe_3O_4$@cellulase. Due to the near-zero values of remanence (Mr) and coercivity (Hc), it is probable that the superparamagnetic nanoparticles exhibited magnetic properties [50, 51].

Figure 5 displays the results on the dimensions of magnetic nanoparticles and chitosan functionalized magnetic nanomaterials in morphological analysis. All particles have dimensions in the nanoscale, having a diameter that falls within the range of 20–40 nm. The size of the $Cs@Fe_3O_4$ nanoscale is 42.2 nm and 36.5 nm, while the size of the Fe_3O_4 NPs is 31.2 nm and 27.5 nm. FESEM results for $Cs@Fe_3O_4$, demonstrates that the chitosan coating on the Fe_3O_4 NPs assists in a rise in the size of the nanoparticles. The application of a chitosan shell resulted in a decrease in the magnetic properties of the nanoparticles and an increase in the repulsive force between them [52]. Consequently, the particles exhibited a more uniform dispersion following the coating, compared to their behavior under circumstances of Fe_3O_4 [53]. The manipulation of surface charges in magnetic nanoparticles enables the regulation of their magnetic attraction, which may be ascertained by measuring their zeta potential, as shown in Fig. 6. In contrast to the Fe_3O_4 nanoparticles, which exhibit a zeta potential of +51 mV, $Cs@Fe_3O_4$ is observed to possess a larger positive charge of +60 mV. This may be due to the hydrogen in chitosan's amino group ($–NH_2$). As a result, this demonstrated that the alteration of Fe_3O_4 NPs with Cs was effective [54].

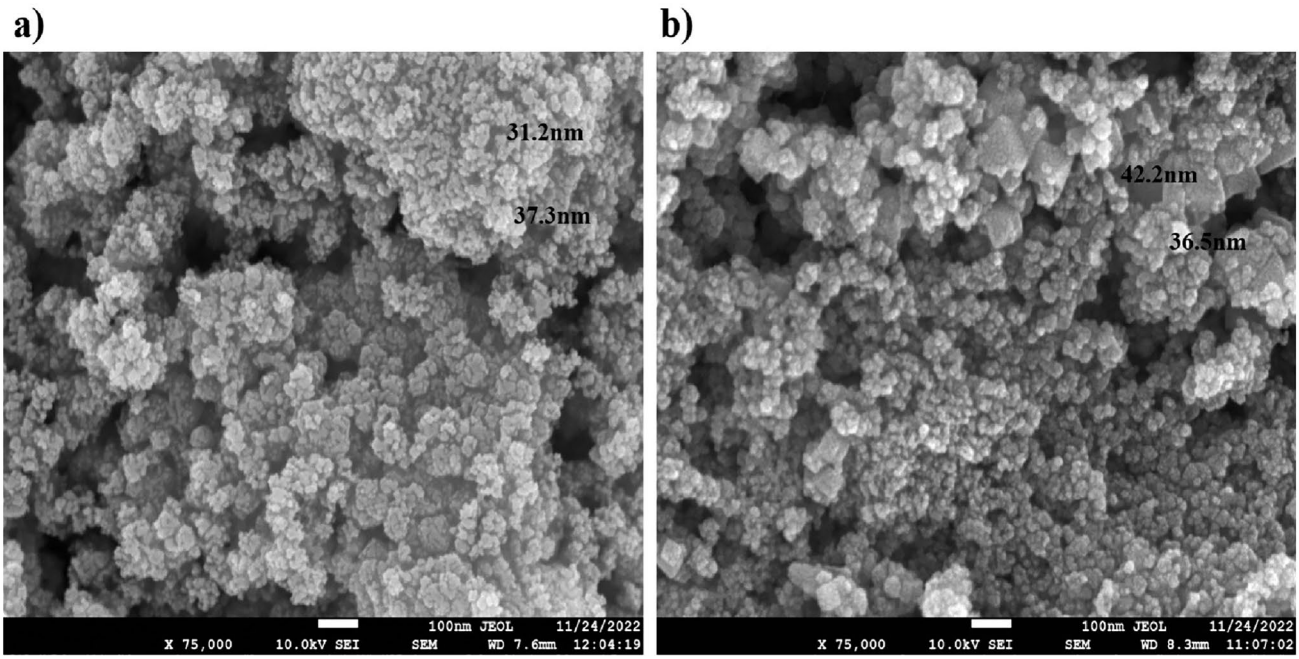

Fig. 5 FESEM images of (**a**) Fe_3O_4 and (**b**) $Cs@Fe_3O_4$ nanocomposites

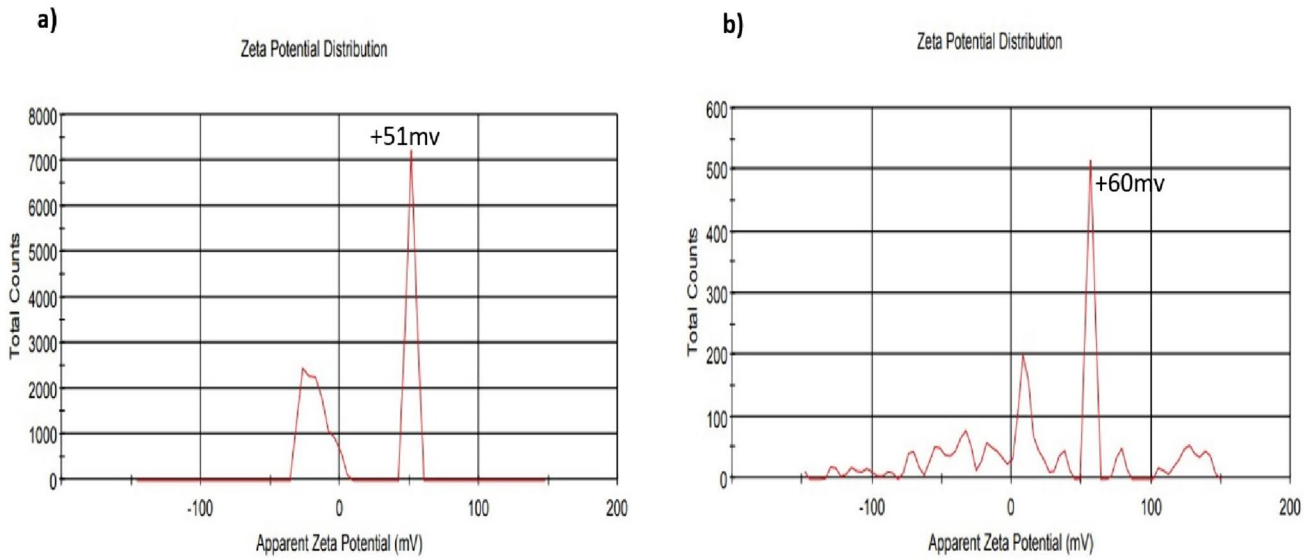

Fig. 6 Zeta Potential of (**a**) Fe_3O_4 and (**b**) $Cs@Fe_3O_4$

Immobilization analysis

Bradford assay was used to determine the enzyme loading capacity. The enzyme loading capacity was increased after Fe_3O_4 were modified with chitosan. This composite synthesis aided the $Cs@Fe_3O_4$ by increasing surface area and boosting enzyme entrapment on its porous surface. Modified chitosan helps prevent the microbiological impact on the enzyme that has been immobilized. The study illustrates that maximum enzyme loading at optimum pH and temperature was 98.07%, with a recovery ratio of 71.67%. Similar findings by John et al. [55] suggest the maximum % enzyme loading of 86% on chitosan-coated Fe_3O_4 nanoparticles.

Optimum pH and temperature

Using a DNS assay with a 1% cellulose substrate, we investigated how pH affected and stabilized the catalytic activity of free and immobilized cellulase. The pH ranged from 4 to 8, as demonstrated in Fig. 7a, both immobilized and free enzymes performed best at pH 5.0 and 7. Immobilized enzymes often outperform unbound enzymes, retaining 96.3% of their activity at pH 5. At pH 7, the immobilized enzyme shows its highest relative activity at 100%, whereas the free enzyme retains only 85.3%. With a predetermined immobilization time (24–72 h), the immobilized enzyme shows its high relative activity (from 87.6% to 100%) when pH is lower from 8 to 7 in 48 h of duration. In contrast, free cellulase exhibits 85.3% activity in 36 h at pH 6, which is the maximum for free enzyme. In immobilization, the pH and the enzyme support ratio seemed to play a significant role. Nevertheless, time of stability has not much impact on its process. Notably, immobilized enzymes typically demonstrate greater activity across a broad pH value scale than free enzymes, indicating that immobilized enzymes possess favorable pH adaptability.

The study investigated the influence of temperature range (50–90 °C) on activity within the pH of 5 and 7. Figure 7b indicates that the immobilized and free enzymes performed optimally at 80 ℃ and 60 ℃. At a temperature of 60 °C, the free enzymes exhibited greater activity than the immobilized enzymes and retained a lower activity of 45.5% at 90 ℃. Further, immobilized enzyme showed maximum activity of 100% at 80 ℃ and when rise in temperature from 10 ℃ i.e., 90 ℃ it retains nearly 73.9% of relative activity. Similar findings by John et al. [55] suggested that immobilized cellulase acquired the highest activity at 80 ℃. At temperatures surpassing 80 ℃, the immobilized cellulase demonstrated greater activity than the loose cellulase, indicating that the immobilized cellulase had enhanced heat resistance compared to the free cellulase [56, 57].

Thermal stability

Considering the industrial utilization of immobilized enzymes, it is crucial to consider thermal equilibrium as a significant component. Figure 8 shows the curve of the thermal stability of both free and immobilized cellulase at 60 °C for 5 h. A temperature of 60 °C, 10° higher than the ideal temperature, was selected briefly to compare the thermal stability. The change in the thermal optimal indicated that the

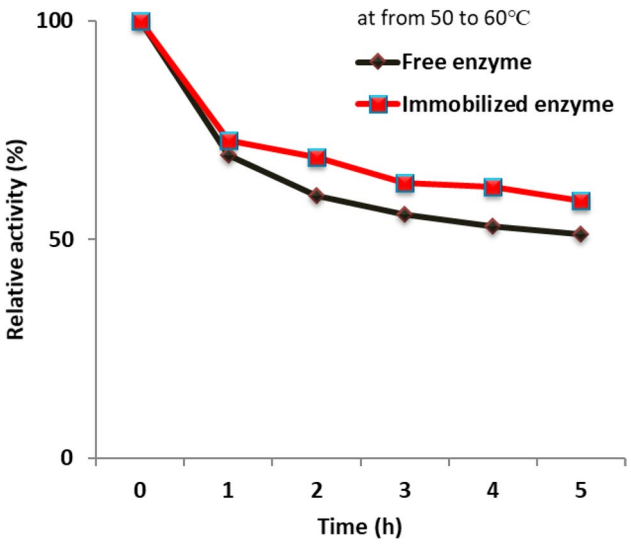

Fig. 8 Effect of thermal stability on free and immobilized enzymes

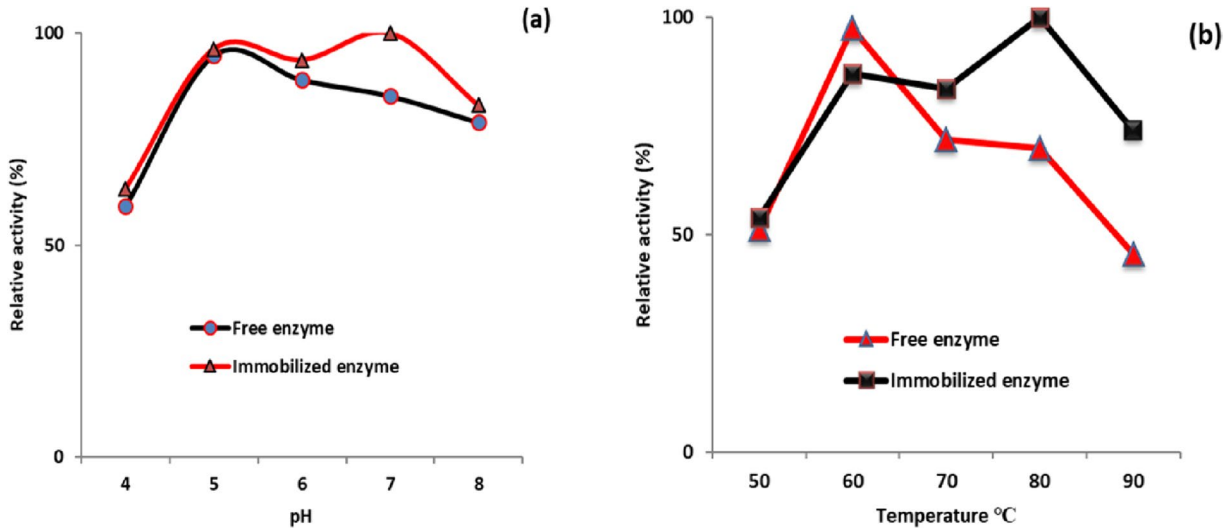

Fig. 7 Influence of (**a**) pH and (**b**) temperature on the relative activity of the immobilized and free enzyme

Table 1 Enzyme kinetics parameters for both free and immobilized cellulase

Enzyme	K_m (mM)	V_{max} (μmol min^{-1} mg^{-1})	R^2	K_{cat} (s^{-1})
Free cellulase	4.718 ± 0.49	29.0 ± 1.518	0.97	0.93
Immobilized cellulase	2.569 ± 0.522	27.03 ± 2.02	0.99	0.87

support matrices in IMC (immobilized cellulase) could retain the tertiary framework of the enzyme. The graph demonstrates that the thermal stability of free and immobilized cellulase decreases. By the end of the fifth hour, the graph shows a significant difference between the two types of cellulase: free cellulase had 50.2% residual activity, and immobilized cellulase had 59.6%. As this study shows the high stability of free and immobilized enzyme in 5 h at 60 ℃, for long duration i.e., 48 h stability of enzyme, it seems there would be minimal impact of long duration time on relative activity. Consistent with earlier research by Pandey and Negi [58], our findings established 60 °C as the temperature optimum for immobilized cellulase and used that cellulase enzyme in lowering the saccharification cost during hydrolysis for successive generation of biofuel with high reusability of cellulase.

Enzyme kinetics study

To study the immobilized and free enzyme's kinetic variable, a Lineweaver–Burk plot was created using a CMC as substrate level range of 0.5–2.5 mg/mL. The Kinetics parameters of free and immobilized enzyme were display in Table 1. The free cellulase enzyme with the loading of 100% on substrate showing Michaelis constant (K_m); 4.718 ± 0.49 mM, with the maximal velocity (V_{max}) of 29.0 ± 1.518 μmol min^{-1} mg^{-1} and K_{cat}; 0.93 s^{-1}, whereas immobilized enzyme showing 2.569 ± 0.522 mM K_m, with 27.03 ± 1.518 μmol min^{-1} mg^{-1} V_{max} and 0.87 s^{-1} K_{cat}. The term "V_{max}" refers to the highest velocity when all the cellulase enzyme's active regions are attached to the CMC substrate. K_{cat} represents the rate of catalytic activity per unit time in an enzyme's kinetic cycle. K_m represents the enzyme's attraction to the CMC substrate Paulraj et al. [59]. When cellulase is immobilized in a magnetic nanomaterial, the V_{max} and K_m values decline, indicating that the enzymes have a stronger binding affinity for the CMC substrate as shown in Table 1. Steric hindrance has been reduced, leading to this greater affinity. Steric hindrance, which slows the dispersion of the precursor and product over time, reduces enzyme binding on the nanomaterial and may affect the enzyme–substrate affinity. Reducing steric hindrance significantly impacts enzyme kinetics Xia et al. [60]. Free enzymes have a larger K_m value, indicating reduced binding capacity to the substrate than immobilized enzymes. The enzyme kinetics of immobilized and free cellulase enzymes are display in Fig. 9 by Lineweaver–Burk plot (LB).

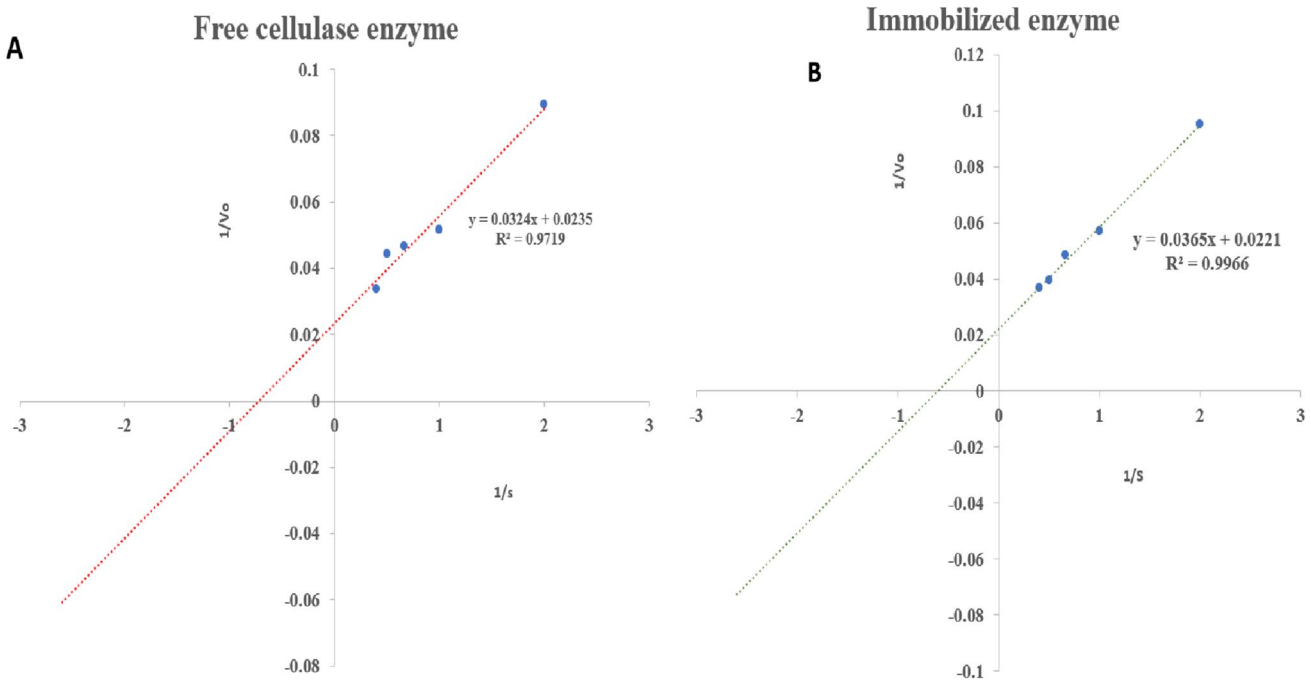

Fig. 9 Lineweaver–Burk plot for (**a**) free enzyme and (**b**) immobilized enzyme

Table 2 Chemical analysis of un-treated and alkali pre-treated sorghum residue

Biomass	Glucan (%)	Hemicellulose (%)	Lignin (%)	Xylan (%)	Moisture content (%)	References
Unprocessed SSR	31.06	28.09	18.7	23.32	9.68	This work
Alkali treated SSR	64.8	11.56	6.4	17.10	13.82	This work
Other research work on sorghum bagasse	30.48–42.65	19.21–29.13	8.40–28.13	21.56	12.15	[61–65]

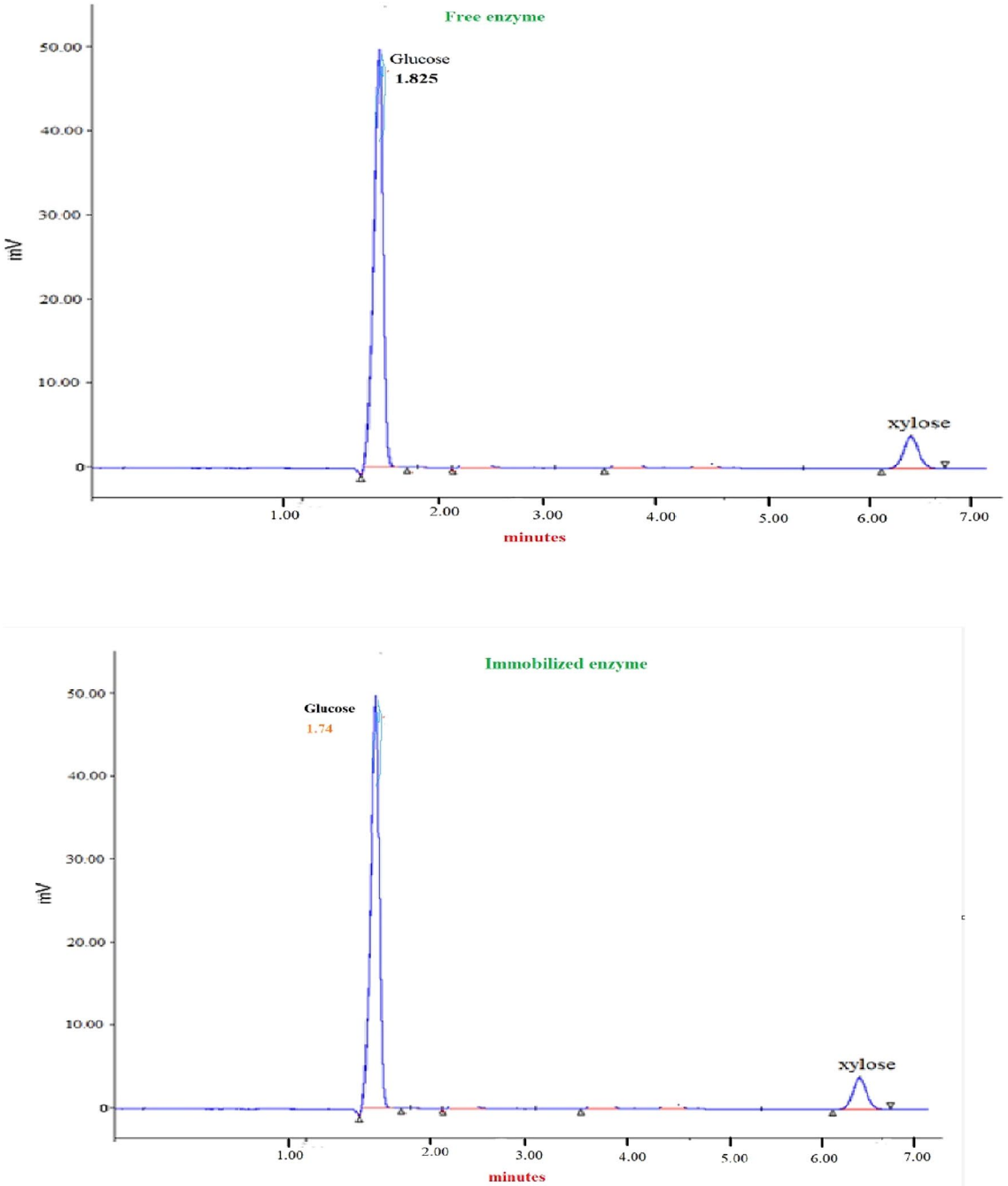

Fig. 10 HPLC analysis of sugars released from sweet sorghum residue with free and immobilized enzyme. The retention time of glucose and xylose peaks was examined at 60 ℃ for up to 7 min. The analysis was conducted in isocratic mode using an amine HPX column with a 1.0 mL/min flow rate

Pre-treatment of sweet sorghum residue

SSR mostly included the bioconversion-critical components of biomass, including lignin, xylan, glucan, and hemicellulose. This work pre-treated the sorghum residue with 2% alkali (NaOH), and dry biomass was used for hydrolysis and saccharification. In the present work, the chemical configuration analysis of pre-treated and un-treated SSR is shown in Table 2.

Hydrolysis and saccharification evaluation

Alkali pre-treated SSR were hydrolyzed with free and cellulase enzymes that would be immobilized on chitosan functionalized iron oxide nanoparticles. Glucose, sucrose and xylose are fermentable sugars generated by the process of hydrolysis, which involves the decomposition of cellulose. When it comes to converting hexose carbohydrates like glucose, the cellulase enzyme utilized throughout the hydrolysis process is considered particularly successful. To estimate the reducing sugars in the saccharification process, the NaOH pre-treated sorghum residue was subjected to analysis using free and immobilized enzymes. The enzyme loading ranged up to 20 g/enzyme unit and was carried out using the One-factor-at-time technique. The optimal temperature for enzymatic hydrolysis is 50 ℃, and the reaction was achieved in a 200 mL flask at 150 rpm.

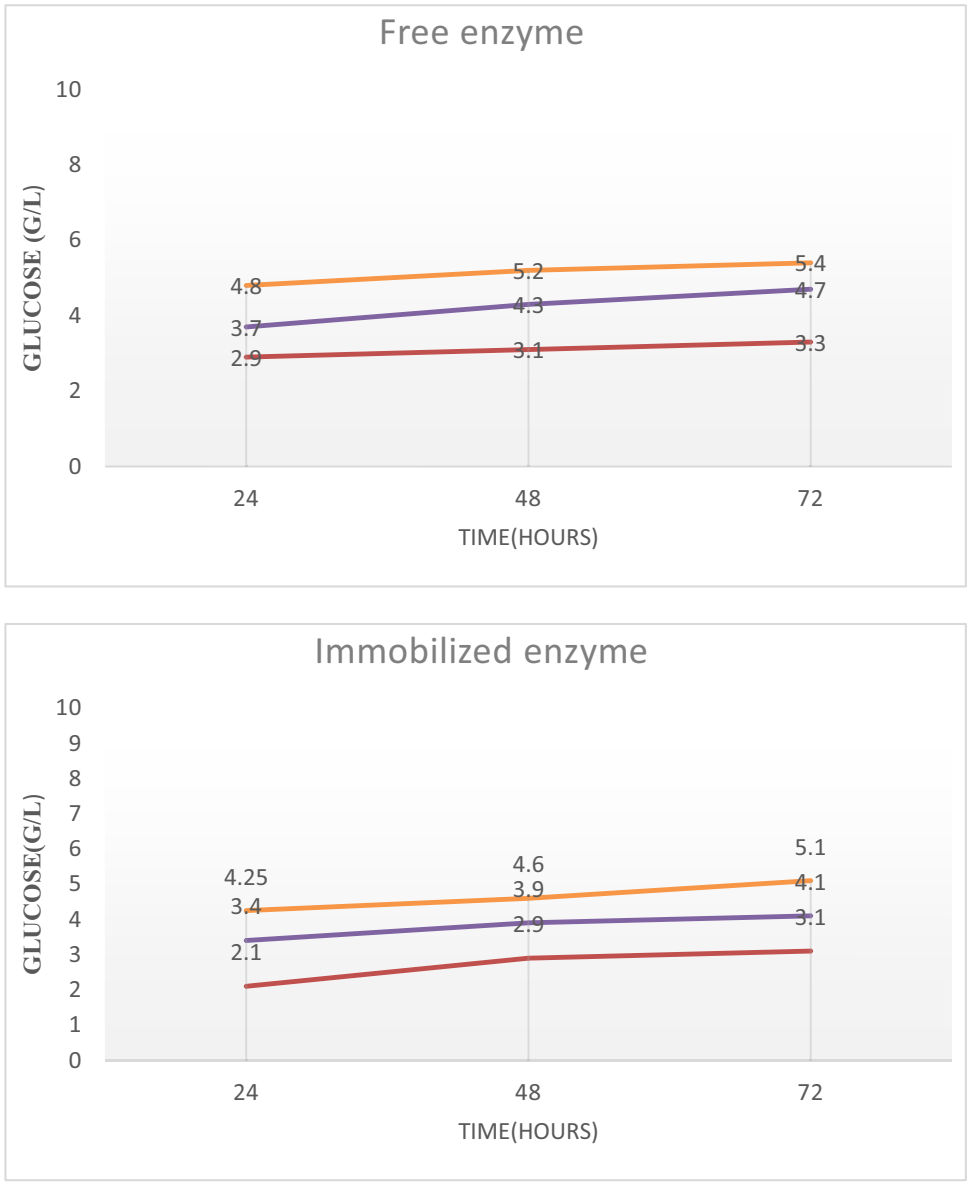

Fig. 11 Glucose concentration from alkali treated biomass with free enzyme and immobilized enzyme

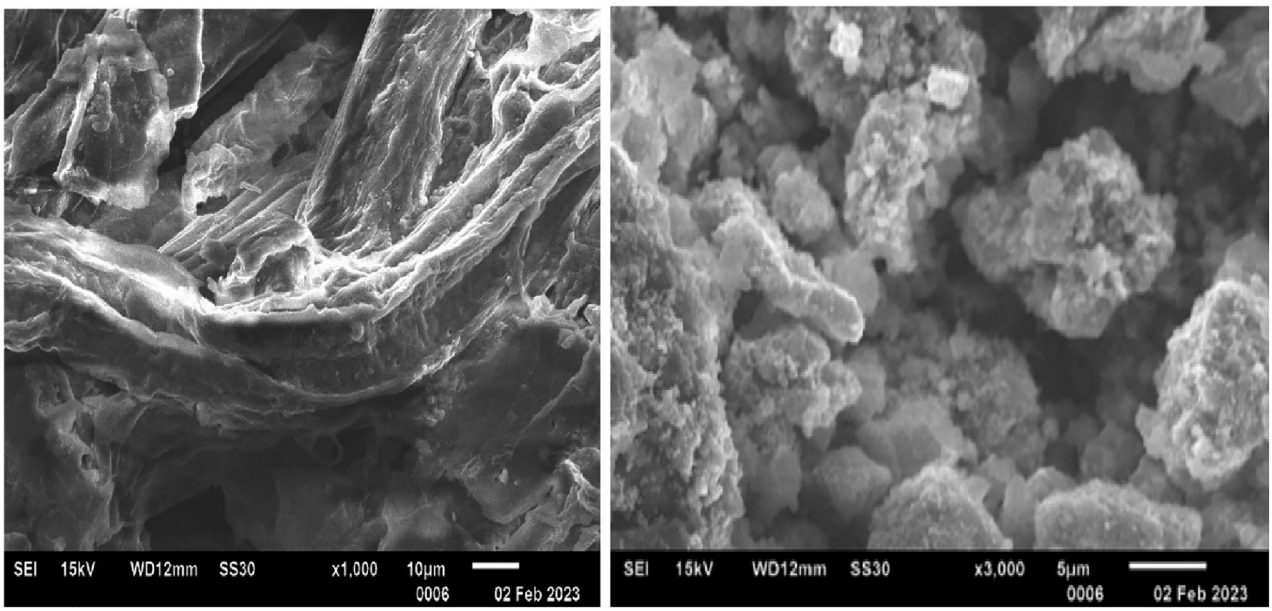

Fig. 12 SEM image of hydrolysis of sorghum residue (**left side**) with free cellulase enzyme (**right side**) with immobilized enzyme of $Cs@Fe_3O_4$

The cellulase activity of 87 FPU/mL was measured. The glucose was determined by centrifuging the hydrolysate after enzymatic hydrolysis at 6000 rpm for 7 min. The fermentable sugars acquired possess further utility in the production of biofuels. The reducing sugars of both the unbound and immobilized enzymes were analyzed using HPLC, as seen in Fig. 10.

The enzyme concentration positively affects the rate of sugar release following hydrolysis. At 20 g/enzyme unit substrate, the enzyme was almost at its optimal concentration, as literature suggests when we doubled the substrate concentration, the hydrolysis process rate was significantly affected.

At 20 g/enzyme unit substrate, *S. cerevisiae* produces the greatest fermentation byproducts, the majority of which are glucose, Fig. 11a, b show the release of glucose concentration at 5, 10, and 20 g/enzyme unit substrate enzymes loading. It predicts that at 20 g/enzyme unit substrate and 3rd day or 72 h, maximum concentration of glucose releases 5.42 g/L with free enzyme and 5.12 g/L with immobilized enzyme with optimum conditions of 50 ℃ and at higher enzyme loading substrate, the residual solids concentration also decline. As a result, 20 g/enzyme unit substrate was determined to be an optimum enzyme concentration for releasing glucose sugar. Similar results were shown by Sánchez-Ramírez et al. [47], in which maximum glucose concentration as reducing sugars released 5.74 g/L for free enzyme and 5.33 g/L for immobilized enzyme for agave fiber hydrolysis. SEM morphology analysis of hydrolysis of sorghum residue with free cellulase and immobilized cellulase on $Cs@Fe_3O_4$ displayed in Fig. 12 shows the validity of the feedstock's breakdown, indicating successful hydrolysis.

Conclusion

This research aimed to create stable magnetic nanoparticles by co-precipitation method and modified with chitosan that can contain cellulase enzyme, which immobilized via covalent bonding. The immobilization efficiency of cellulase enzyme on $Cs@Fe_3O_4$ was 98.07%, with a recovery ratio of 71.67% attributed to pH 5 at 50 ℃. The most relevant process occurs when nanoparticles are easily separated with a magnetic field that allows these enzymes to be reused for biomass hydrolysis. This study also signifies that 2% NaOH concentration obtain the highest concentration of cellulose 64.8%, and 67.5% reduction in lignin content. Under optimum parameters, at 20 FPU/g substrate and 3rd day or 72 h, the maximum concentration of glucose releases 5.42 g/L with free enzyme and 5.12 g/L with immobilized enzyme with 50 ℃. This research aims to evaluate the comparison of releasing reducing sugar such as glucose from sorghum residue with immobilized enzyme from free cellulase, which is a cost-effective and environmentally sustainable process. Overall, this endeavor prevents contamination of the environment and provides reducing sugar for bioenergy through the biodegradation of sorghum biomass.

Acknowledgements The authors are thankful to the Department of Environmental Science and Engineering, Guru Jambheshwar University of Science and Technology, Hisar, Haryana, India for providing multiple facilities for conducting this research.

Author contributions PP and LS conceptualized the presented data. Pallavi performed all experiments, methodology and results under the supervision of Lakhvinder Singh. Pallavi wrote the manuscript with

the contribution of Lakhvinder Singh. All authors discussed the results and contributed to the final manuscript.

Funding There was no specific funding source for this conducted research work.

Data availability Data will be made available on request.

Declarations

Conflict of interests The authors declare no competing interests.

References

1. Rose PK (2022) Bioconversion of agricultural residue into biofuel and high-value biochemicals: recent advancement. In: Zero waste biorefinery. Springer Nature Singapore, Singapore, pp. 233–268. https://doi.org/10.1007/978-981-16-8682-5_9
2. Stamenkoviić OS, Siliveru K, Veljković VB, Banković-Ilić IB, Tasić MB, Ciampitti IA, Dalović IG, Mitrović PM, Sikora VS, Prasad PVV (2020) Production of biofuels from sorghum. Renew Sustain Energy Rev 124:109769. https://doi.org/10.1016/j.rser.2020.109769
3. Zabed H, Sahu JN, Suely A, Boyce AN, Faruq G (2017) Bioethanol production from renewable sources: current perspectives and technological progress. Renew Sustain Energy Rev 71:475–501. https://doi.org/10.1016/j.rser.2016.12.076
4. Klasson KT, Boone SA (2021) Bioethanol fermentation of clarified sweet sorghum (*Sorghum bicolor* (L.) *Moench*) syrups sealed and stored under vegetable oil. Ind Crop Prod 163:113330. https://doi.org/10.1016/j.indcrop.2021.113330
5. Yucel C, Dweikat I, Yucel D, Gultekin R (2020) Bioethanol potential of different sweet sorghum genotypes grown under Mediterranean conditions. Fresenius Environ Bull 29(12):10356–10365
6. Sipos B, Réczey J, Somorai Z, Kádá Z, Dienes D, Réczey K (2009) Sweet sorghum as feedstock for ethanol production: enzymatic hydrolysis of steam-pretreated bagasse. Appl Biochem Biotechnol 153(1–3):151–162
7. Zhang C, Wen H, Chen C, Cai D, Fu C, Li P, Qin P, Tan T (2019) Simultaneous saccharification and juice co-fermentation for high-titer ethanol production using sweet sorghum stalk. Renew Energy 134:44–53. https://doi.org/10.1016/j.renene.2018.11.005
8. Sheikh ZUD, Bajar S, Devi A, Rose PK, Suhag M, Yadav A, Yadav DK, Deswal T, Kaur J, Kothari R, Pathania D (2023) Nanotechnology based technological development in biofuel production: current status and future prospects. Enzyme Microbial Technol 110304. https://doi.org/10.1016/j.enzmictec.2023.110304
9. Verma ML, Kumar P, Chandel H (2023) Nanobiotechnological routes in lignocellulosic waste pre-treatment for bio-renewables production. In: Gakkhar N, Kumar S, Sarma AK, Graham NT (eds) Recent advances in bio-energy research. ICRABR-2022 2022. Springer proceedings in energy. Springer, Singapore. https://doi.org/10.1007/978-981-99-5758-3_3
10. Rose PK, Dhull SB, Kidwai MK (2022) Cultivation of wild mushrooms using lignocellulosic biomass-based residue as a substrate. In: Wild mushrooms. CRC Press, pp. 493–520
11. Zhao X, Zhang L, Liu D (2012) Biomass recalcitrance. Part I: The chemical compositions and physical structures affecting the enzymatic hydrolysis of lignocellulose. Biofuel Bioprod Bior 6(4):465–482
12. Rose PK, Poonia V, Kumar R, Kataria N, Sharma P, Lamba J, Bhattacharya P (2023) Congo red dye removal using modified banana leaves: adsorption equilibrium, kinetics, and reusability analysis. Groundw Sustain Dev 23:101005. https://doi.org/10.1016/j.gsd.2023.101005
13. Rose PK, Kumar R, Kumar R, Kumar M, Sharma P (2023) Congo red dye adsorption onto cationic amino-modified walnut shell: characterization, RSM optimization, isotherms, kinetics, and mechanism studies. Groundw Sustain Dev 21:100931. https://doi.org/10.1016/j.gsd.2023.100931
14. Rahikainen JL, Martin-Sampedro R, Heikkinen H, Rovio S, Marjamaa K, Tamminen T (2013) Inhibitory effect of lignin during cellulose bioconversion: the effect of lignin chemistry on non-productive enzyme adsorption. Bioresour Technol 133:270–278
15. Ávila PF, de Mélo AH, Goldbeck R (2023) Cello-oligosaccharides production from multi-stage enzymatic hydrolysis by lignocellulosic biomass and evaluation of prebiotic potential. Innov Food Sci Emerg Technol 85:103335
16. Xu C, Tong S, Sun L, Gu X (2023) Cellulase immobilization to enhance enzymatic hydrolysis of lignocellulosic biomass: an all-inclusive review. Carbohydr Polym 121319. https://doi.org/10.1016/j.carbpol.2023.121319
17. Revathi D, Ramalingam S (2023) A study on critical associations of media components on enhanced cellulase production from wild *Trichoderma viride* and cellulase immobilization on iron-oxide magnetic nanoparticles. J Environ Biol 44(1):27–33. https://doi.org/10.22438/jeb/441/MRN-5048
18. Sulman AM, Grebennikova OV, Karpenkov AY, Tikhonov BB, Molchanov VP, Matveeva VG et al (2023) Magnetic nanobiocatalysts based on immobilized cellulase. Chem Eng Trans 103:793–798. https://doi.org/10.3303/CET23103133
19. Verma ML, Barrow CJ (2015) Recent advances in feedstocks and enzyme-immobilised technology for effective transesterification of lipids into biodiesel. In: Kalia V (ed) Microbial factories. Springer, New Delhi. https://doi.org/10.1007/978-81-322-2598-0_6
20. Verma ML, Dhanya BS, Wang B, Thakur M, Rani V, Kushwaha R (2024) Bio-Nanoparticles mediated transesterification of algal biomass for biodiesel production. Sustainability 16:295. https://doi.org/10.3390/su16010295
21. Verma ML, Barrow CJ, Puri M et al (2013) Nanobiotechnology as a novel paradigm for enzyme immobilization and stabilization with potential applications in biodiesel production. Appl Microbiol Biotechnol 97:23–39
22. Galodiya MN, Chakma S (2024) Immobilization of enzymes on functionalized cellulose nanofibrils for bioremediation of antibiotics: degradation mechanism, kinetics, and thermodynamic study. Chemosphere 349:140803. https://doi.org/10.1016/j.chemosphere.2023.140803
23. Li C, Jiang S, Zhao X, Liang H (2017) Co-immobilization of enzymes and magnetic nanoparticles by metal-nucleotide hydrogel nanofibers for improving stability and recycling. Molecules 22:179. https://doi.org/10.3390/molecules22010179
24. Elamin NY, Modwi A, Abd El-Fattah W, Rajeh A (2023) Synthesis and structural of Fe_3O_4 magnetic nanoparticles and its effect on the structural optical, and magnetic properties of novel poly (methyl methacrylate)/polyaniline composite for electromagnetic and optical applications. Opt Mater 135:113323. https://doi.org/10.1016/j.optmat.2022.113323
25. Bilal M, Ashraf SS, Ferreira LFR, Cui J, Lou WY, Franco M (2020) Nanostructured materials as a host matrix to develop robust peroxidases-based nano biocatalytic systems. Int J Biol Macromol 162:1906–1923
26. Narisetty V, Tarafdar A, Bachan N, Madhavan A, Tiwari A, Chaturvedi P, Sindhu R (2023) An overview of cellulase immobilization strategies for biofuel production. BioEnergy Res 16(1):4–15

27. Nayeri MD, Nikkhah H, Zilouei H, Bazarganipour M (2023) Immobilization of cellulase on graphene oxide coated with $NiFe_2O_4$ and Fe_3O_4 for hydrolysis of rice straw. Cellulose 30(9):5549–5571. https://doi.org/10.1007/s10570-023-05207-7
28. Behshad Y, Pazhang M, Najavand S, Sabzi M (2023) Enhancing enzyme stability and functionality: covalent immobilization of trypsin on magnetic gum arabic modified Fe_3O_4 nanoparticles. Appl Biochem Biotechnol 1–18. https://doi.org/10.1007/s12010-023-04830-1
29. Ismail AM, Tiama TM, Farghaly A, Elhaes H, Ibrahim MA (2023) Assessment of the functionalization of chitosan/iron oxide nanoparticles. Biointerface Res Appl Chem 13(6):582
30. Kaur G, Taggar MS, Kalia A (2023) Cellulase-immobilized chitosan-coated magnetic nanoparticles for saccharification of lignocellulosic biomass. Environ Sci Pollut Res 1–21. https://doi.org/10.1007/s11356-023-27919-w
31. Verma ML, Dhanya BS, Rani V, Thakur M, Jeslin J, Kushwaha R (2020) Carbohydrate and protein based biopolymeric nanoparticles: current status and biotechnological applications. Int J Biol Macromol 154:390–412. https://doi.org/10.1016/j.ijbiomac.2020.03.105
32. Xu X, Chen T, Xu L, Lin J (2024) Immobilization of laccase on magnetic nanoparticles for enhanced polymerization of phenols. Enzyme Microb Technol 172:110331. https://doi.org/10.1016/j.enzmictec.2023.110331
33. Asar MF, Ahmad N, Husain Q (2020) Chitosan modified Fe_3O_4/graphene oxide nanocomposite as a support for high yield and stable immobilization of cellulase: its application in the saccharification of microcrystalline cellulose. Prep Biochem Biotechnol 50(5):460–467. https://doi.org/10.1080/10826068.2019.1706562
34. Verma ML, Sukriti Dhanya BS (2022) Synthesis and application of graphene-based sensors in biology: a review. Environ Chem Lett 20:2189–2212. https://doi.org/10.1007/s10311-022-01404-1
35. Ansari SA, Damanhory AA (2023) Biotechnological application of Aspergillus oryzae β-galactosidase immobilized on glutaraldehyde modified zinc oxide nanoparticles. Heliyon 9(2). https://doi.org/10.1016/j.heliyon.2023.e13089
36. Verma ML, Kumar S, Das A, Randhawa JS, Chamundeeswari M (2019) Enzyme immobilization on chitin and chitosan-based supports for biotechnological applications. In: Crini G, Lichtfouse E (eds) Sustainable agriculture reviews 35. Sustainable agriculture reviews, vol. 35. Springer, Cham. https://doi.org/10.1007/978-3-030-16538-3_4
37. Sharma B, Larroche C, Dussap CG (2020) Comprehensive assessment of 2G bioethanol production. Bioresour Technol 313:123630. https://doi.org/10.1016/j.biortech.2020.123630
38. Wirawan F, Cheng C-L, Lo Y-C, Chen C-Y, Chang J-S, Leu S-Y (2020) Continuous cellulosic bioethanol co-fermentation by immobilized *Zymomonas mobilis* and suspended *Pichia stipitis* in a two-stage process. Appl Energy 266:114871
39. Xie WL, Wang JL (2012) Immobilized lipase on magnetic chitosan microspheres for transesterification of soybean oil. Biomass Bioenerg 36:373–380
40. Zang L, Qiu J, Wu X, Zhang W, Sakai E, Wei Y (2014) Preparation of magnetic chitosan nanoparticles as support for cellulase immobilization. Ind Eng Chem Res 53:3448–3454
41. Ghose TK (1987) Measurement of cellulose activities. Pure Appl Chem 59(2):257–268
42. Selvarajan E, Mohanasrinivasan V (2015) Kinetic studies on exploring lactose hydrolysis potential of β galactosidase extracted from *Lactobacillus plantarum* HF571129. J Food Sci Technol 52:6206–6217
43. Punia P, Singh L (2024) Optimization of alkali pre-treatment of sweet sorghum [*Sorghum bicolor* (L.) *Moench*] residue to improve enzymatic hydrolysis for fermentable sugars. Waste Manage Bullet 2(1):131–141. https://doi.org/10.1016/j.wmb.2023.12.007
44. Sluiter A, Hames B, Ruiz R, Scarlata C, Sluiter J, Templeton D, Crocker DLAP (2008) Determination of structural carbohydrates and lignin in biomass. Lab Anal Proc 1617(1):1–16
45. Trifoi AR, Matei E, Râpă M, Berbecaru AC, Panaitescu C, Banu I, Doukeh R (2023) Coprecipitation nanoarchitectonics for the synthesis of magnetite: a review of mechanism and characterization. React Kinet Mech Catal 136(6):2835–2874. https://doi.org/10.1007/s11144-023-02514-9
46. Sodipo BK, Noqta OA, Aziz AA, Katsikini M, Pinakidou F, Paloura EC (2023) Influence of capping agents on fraction of Fe atoms occupying octahedral site and magnetic property of magnetite (Fe_3O_4) nanoparticles by one-pot co-precipitation method. J Alloy Compd 938:168558. https://doi.org/10.1016/j.jallcom.2022.168558
47. Sanchez-Ramirez J, Martinez-Hernandez JL, Segura-Ceniceros P, Lopez G, Saade H, Medina-Morales MA, Ilyina A (2017) Cellulases immobilization on chitosan-coated magnetic nanoparticles: application for Agave Atrovirens lignocellulosic biomass hydrolysis. Bioprocess Biosyst Eng 40:9–22
48. Ding Yongling, Shirley Z. Shen, Huadong Sun, Kangning Sun, Futian Liu, Yushi Qi, Jun Yan (2015) Design and construction of polymerized-chitosan coated Fe_3O_4 magnetic nanoparticles and its application for hydrophobic drug delivery. Mater Sci Eng C 487–498. https://doi.org/10.1016/j.msec.2014.12.036
49. Karimova A, Shirinova H, Nargiz G, Nuriyeva S, Gahramanli L (2023) Preparation and characterization of magnetic iron oxide (Fe_3O_4) nanoparticles with different polymer coating agents
50. Kneller EF, Luborsky FE (1963) Particle size dependence of coercivity and remanence of single-domain particles. J Appl Phys 34:656–658. https://doi.org/10.1063/1.1729324
51. Kim DK, Zhang Y, Voit W, Rao KV, Muhammed M (2001) Synthesis and characterization of surfactant-coated superparamagnetic monodispersed iron oxide nanoparticles. J Magn Magn Mater 225:30–36. https://doi.org/10.1016/s0304-8853(00)01224-5
52. Podrepšek GH, Knez Z, Leitge M (2020) Development of chitosan functionalized magnetic nanoparticles with bioactive compounds. Nanomaterials 10:1913. https://doi.org/10.3390/nano10101913
53. Kuo CH, Liu YC, Chang CM, Chen JH, Chang C, Shieh CJ (2012) Optimum conditions for lipase immobilization on chitosan-coated Fe_3O_4 nanoparticles. Carbohydr Polym 87:2538–2545
54. Shanmugam S, Krishnaswamy S, Chandrababu R, Veerabagu U, Pugazhendhi A, Mathimani T (2020) Optimal immobilization of *Trichoderma asperellum* laccase on polymer coated Fe_3O_4@ SiO_2 nanoparticles for enhanced biohydrogen production from delignified lignocellulosic biomass. Fuel 273:117777
55. John JA, Samuel MS, Selvarajan E (2023) Immobilized cellulase on Fe_3O_4/GO/CS nanocomposite as a magnetically recyclable catalyst for biofuel application. Fuel 333:126364
56. Ladole MR, Pokale PB, Varude VR, Belokar PG, Pandit AB (2021) One pot clarification and debittering of grapefruit juice using co-immobilized enzymes@ chitosan MNPs. Int J Biol Macromol 167:1297–1307
57. Chen Q, Liu D, Wu C, Yao K, Li Z, Shi N (2018) Co-immobilization of cellulase and lysozyme on amino-functionalized magnetic nanoparticles: an activity-tunable biocatalyst for extraction of lipids from microalgae. Bioresour Technol 263:317–324
58. Pandey AK, Negi S (2020) Enhanced cellulase recovery in SSF from *Rhizopus oryzae* SN5 and immobilization for multi-batch saccharification of carboxymethylcellulose. Biocatal Agric Biotechnol 26:101656
59. Paulraj Gundupalli M, Sahithi STA, Cheng Y-S, Tantayotai P, Sriariyanun M (2021) Differential effects of inorganic salts on

cellulase kinetics in enzymatic saccharification of cellulose and lignocellulosic biomass. Bioprocess Biosyst Eng 44:2331–2344
60. Xia T-T, Liu C-Z, Hu J-H, Guo C (2016) Improved performance of immobilized laccase on amine-functioned magnetic Fe_3O_4 nanoparticles modified with polyethylenimine. Chem Eng J 295:201–206
61. Wen H, Chen H, Cai D, Gong P, Zhang T, Wu Z, Tan T (2018) Integrated in situ gas stripping–salting-out process for high-titer acetone–butanol–ethanol production from sweet sorghum bagasse. Biotechnol Biofuels 11:1–12. https://doi.org/10.1186/s13068-018-1137-5
62. Thanapimmetha A, Saisriyoot M, Khomlaem C, Chisti Y, Srinophakun PA (2019) Comparison of methods of ethanol production from sweet sorghum bagasse. Biochem Eng J 151:107352. https://doi.org/10.1016/j.bej.2019.107352
63. Su C, Qi L, Cai D, Chen B, Chen H, Zhang C, Si Z, Wang Z, Li G, Qin P (2020) Integrated ethanol fermentation and acetone-butanol-ethanol fermentation using sweet sorghum bagasse. Renew Energy 162:1125–1131. https://doi.org/10.1016/j.renene.2020.07.119
64. Loku UA, Ruplal C, Yanna L, John H, Watson DG (2015) Laboratory scale optimization of alkali pretreatment for improving enzymatic hydrolysis of sweet sorghum bagasse. Ind Crops Prod 74:977–986. https://doi.org/10.1016/j.indcrop.2015.05.044
65. Martins RP, Schmatz AA, de Freita LA, Mutton MJR, Brienzo M (2021) Solubilization of hemicellulose and fermentable sugars from bagasse, stalks, and leaves of sweet sorghum. Ind Crops Prod 170:113813